Check for updates

Antinociceptive Activity of *Borreria verticillata*: *In vivo* and *In silico* Studies

Rosa H. M. Silva[1]*, Nathália de Fátima M. Lima[1], Alberto J. O. Lopes[1],
Cleydlenne C. Vasconcelos[1], José W. C. de Mesquita[2], Ludmilla S. S. de Mesquita[2],
Fernando C. V. M. Lima[1], Maria N. de S. Ribeiro[2], Ricardo M. Ramos[3],
Maria do Socorro de S. Cartágenes[1]* and João B. S. Garcia[4]*

[1] Experimental Study of Pain Laboratory, Department of Physiological Sciences, Federal University of Maranhão, São Luís, Brazil, [2] Laboratory of Pharmacognosy, Department of Pharmacy, Federal University of Maranhão, São Luís, Brazil, [3] Research Laboratory Information Systems, Department of Information, Environment, Health and Food Production, Federal Institute of Piauí, Teresina, Brazil, [4] Experimental Study of Pain Laboratory, Department of Pain and Palliative Care, Federal University of Maranhão, São Luís, Brazil

Borreria verticillata (L.) G. Mey. known vassourinha has antibacterial, antimalarial, hepatoprotective, antioxidative, analgesic, and anti-inflammatory, however, its antinociceptive action requires further studies. Aim of the study evaluated the antinociceptive activity of *B. verticillata* hydroalcoholic extract (EHBv) and ethyl acetate fraction (FAc) by *in vivo* and *in silico* studies. *In vivo* assessment included the paw edema test, writhing test, formalin test and tail flick test. Wistar rats and Swiss mice were divided into 6 groups and given the following treatments oral: 0.9% NaCl control group (CTRL), 10 mg/kg memantine (MEM), 10 mg/kg indomethacin (INDO), 500 mg/kg EHBv (EHBv 500), 25 mg/kg FAc (FAc 25) and 50 mg/kg FAc (FAc 50). EHBv, FAc 25 and 50 treatments exhibited anti-edematous and peripheral antinociceptive effects. For *in silico* assessment, compounds identified in FAc were subjected to molecular docking with COX-2, GluN1a and GluN2B. Ursolic acid (UA) was the compound with best affinity parameters (binding energy and inhibition constant) for COX-2, GluN1a, GluN2B, and was selected for further analysis with molecular dynamics (MD) simulations. In MD simulations, UA exhibited highly frequent interactions with residues Arg120 and Glu524 in the COX-2 active site and NMDA, whereby it might prevent COX-2 and NMDA receptor activation. Treatment with UA 10 mg/Kg showed peripheral and central antinociceptive effect. The antinociceptive effect of *B. verticillata* might be predominantly attributed to peripheral actions, including the participation of anti-inflammatory components. Ursolic acid is the main active component and seems to be a promising source of COX-2 inhibitors and NMDA receptor antagonists.

Keywords: *Borreria verticillata*, COX-2, NMDA receptor, molecular docking, molecular dynamics simulations

INTRODUCTION

Pain is a warning system that informs the body about the occurrence of tissue damage (Nickel et al., 2012). In the pathophysiology of pain several biological actions are involved, including activation of cyclooxygenase 2 enzyme (COX-2) and N-methyl-D-aspartate (NMDA) receptor.

COX-2 is upregulated in the central nervous system in response to inflammatory factors. It is a rate-limiting enzyme for prostanoid production during inflammation

(Ricciotti and Fitzgerald, 2011). Prostaglandin E2, the main pro-inflammatory prostanoid, induces painful hypersensitivity through modulation in the nociceptive pathways, activates the periphery ionic channels such as sodium, calcium, and potentiates the central activation of NMDA and α-amino-3-hydroxy-5-methylsoxazol-4-propionic (AMPA) receptors (Chen et al., 2013). Inhibition of COX-2 enzymatic activity prevents prostanoid production, thus this enzyme is a usual target of non-steroidal anti-inflammatory drugs (NSAIDs) (Zaiss et al., 2014).

The activation of NMDA receptor requires the binding of glycine and glutamate to its subunits GluN1 and GluN2, respectively (Tajima et al., 2016). It is well-known that activation of NMDA receptors causes central sensitization, amplification of spinal nociception, increased ionic conductance and membrane depolarization (Phang and Tan, 2013). For this reason, NMDA receptor antagonists (e.g., memantine) are considered an option in the management of opioid-resistant and chronic pain (Hewitt, 2000).

Therefore, NSAIDs and NMDA receptor antagonists are used to afford pain relief. However, the use of these agents is limited by the occurrence of side effects, such as dizziness, vomiting, constipation, and gastric erosions. These problems and the impact of pain in the quality of life of patients evidence the need of novel therapeutic targets for pain management.

Medicinal plants and their derivatives represent a common alternative for the treatment of diseases (Kandimalla et al., 2016; Zaia et al., 2016). *Borreria verticillata* (L.) G. Mey., known in Brazil as poaia, cordão-de-frade and vassourinha (Júnior et al., 2012) is traditionally used for various therapeutic purposes including the treatment of pain and inflammatory conditions (Vieira et al., 1999; Souza et al., 2013). It has shown to possess antibacterial (Neto et al., 2002; Ogunwande et al., 2010; Balde et al., 2015), hepatoprotective (Murtala et al., 2015), antioxidant (Abdullahi-Gero et al., 2014a), anti-inflammatory and analgesic (Abdullahi-Gero et al., 2014b) activity.

New technologies have been applied to the assessment of the pharmacological properties of extracts and active principles of medicinal plants, such as molecular docking and molecular dynamic, which is a computer-based approach used to give a prediction of the ligand-receptor complex structure (Meng et al., 2011). The combination of computational technique with biological assay became an important strategy toward finding plant-based drugs (Sharma and Sarkar, 2012).

Considering the factors that contribute to the mechanisms of pain and the use of medicinal plants as multi-targets therapeutic alternatives, the aim of the present study was to assess the antinociceptive activity of the crude hydroalcoholic extract and ethyl acetate fraction of *B. verticillata*. Furthermore, evaluate the molecular interactions of compounds present in ethyl acetate fraction with COX-2 enzyme and NMDA receptor.

MATERIALS AND METHODS

Botanic Material

The aerial parts of *Borreria verticillata* (L.) G. Mey, Rubiaceae were collected at São José de Ribamar, Maranhão state,

(2°33′13.3″ S 44°11′22.8″ W), Brazil, in July 2014. A voucher specimen was deposited at Maranhão Herbarium (MAR), of Federal University of Maranhão (UFMA), under the registration number 5151.

Obtaining the Hydroalcoholic Extract and the Ethyl Acetate Fraction

Aerial parts of *B. verticillata* were dried at 38°C in an oven with circulating air and powdered with a knife mill to obtain a moderately coarse powder (particle sizes under 710 μm and over 250 μm). The powder of *B. verticillata* aerial parts was macerated with 70% ethanol for 5 days (this step was repeated 3 times) obtaining a solution. The solution was filtered and concentrated to a small volume at 40°C in a rotary evaporator under vacuum, to obtain the hydroalcoholic extract of *B. verticillata* (EHBv). EHBv was dissolved in methanol:water (70:30,v/v) for 60 min under mechanical agitation, and successively subjected to liquid-liquid extraction with hexane, chloroform, and ethyl acetate. The solutions were filtered and concentrated at 40°C in a rotary evaporator under vacuum, to ethyl acetate fraction (FAc).

Phenolic and Flavonoid Content Assessment

Total phenolic content (TPC) was determined using Folin-Ciocalteu reagent and 20% sodium carbonate. The reaction was kept in the dark for 2 h at room temperature; absorbance was read with a spectrophotometer at 760 nm (Dutra et al., 2014). The PCC was calculated based on the calibration curve plotted with gallic acid standard solutions (1.0–30.0 μg/mL) and is expressed as gallic acid equivalent (mg/mL).

Total flavonoid content (TFC) was determined using a 5% methanol solution of aluminum chloride ($AlCl_3$). The reaction was kept in the dark for 30 min at room temperature; absorbance was read with a spectrophotometer at 425 nm (Dutra et al., 2008). The TFC was calculated based on the calibration curve plotted with quercetin standard solutions (1.0–30.0 μg/mL) and is expressed as quercetin equivalent (mg/mL).

High-Performance Liquid Chromatography with Ultraviolet-Visible Detector (HPLC UV/Vis)

EHBv and FAc were analyzed with an HPLC device (Thermo Finnigan Surveyor) coupled to an ultraviolet-visible detector and a reversed phase ACE C-18 (250 X 4.6 mm, 5 μm) column was used. The components of FAc and EHBv were separated at room temperature through gradient elution at a 1 mL/min flow rate. The mobile phases consisted of purified water with 0.1% acetic acid (A) and acetonitrile (B). The gradient used was as follows: 0–5 min, 20% B; 5–10 min, 25% B; 10–15 min, 25–23% B; 15–20 min, 23–21% B; 20–25 min, 21–18% B; 25–30 min, 18–15% B; 30–35 min, 15–0% B. The injection volume was 5 μL, and UV-Vis detection was performed at 254 nm. The compounds were identified on the basis of co-injection with standards.

Gas Chromatography—Mass Spectrometry (GC-MS)

FAc (10 mg) was derivatized in pyridine (300 μL) and bis-(trimethylsilyl) trifluoroacetamide with trimethylchlorosilane (BSTFA/TMCS, 100 μL) and was heated at 80°C for 1 h. The derivatized product was analyzed with a gas chromatograph (GC-2010, Shimadzu, Japan) coupled to a mass spectrometer (GCMS-QP2010 SE, Shimadzu, Japan) with an Rtx-5MS column (30 m × 0.25 mm ix 0.25 μm, Restek, USA), helium as the carrier gas and a 1.0 mL/min flow rate. The oven temperature was first kept at 70°C and then set to increase 4°C/min until 310°C. The temperature was maintained at 310°C for 4 min. The injector temperature was set to 250°C; the injection volume was 1.0 mL at a 1:30 ratio. The mass spectra were obtained by means of electron impact ionization (70 eV) on total ion scanning mode (40 to 1,000 m/z) with the ion source at 200°C. The compounds were identified through comparison of the obtained mass spectra with the NIST 11 library.

In vivo Biological Studies

Animals

The present study used adult, male and female Wistar *Rattus norvegicus* rats with weights ranging from 200 to 300 g and adult, male, and female *Mus musculus* mice with weights ranging from 25 to 35 g, which were procured from the Central Vivarium (Biotério Central), Federal University of Maranhão (UFMA). Animals were provided with free access to food and water in an environment with controlled temperature and 12/12 h light/dark cycle. This study was carried out in accordance with the recommendations of IASP Guidelines for the Use of Animals in Research. The experimental protocols were approved by the UFMA Ethics in Animal Use Committee (CEUA), ruling no. 17, protocol no. 23115.013545/2015-89.

Experimental Groups

Six experimental groups with 6 animals each were used. CTRL group was treated oral (p.o) with 0.9% NaCl (0.1 mL/kg); the INDO group was treated with indomethacin (10 mg/kg p.o.); MEM group was treated with memantine (10 mg/kg p.o.); FAc groups were treated with fraction the *B. verticillata* at doses of 25 mg/kg p.o (FAc 25) and 50 mg/kg p.o (FAc 50) and the EHBv group was treated with the hydroalcoholic extract of *B. verticillata* (500 mg/kg p.o.). NaCl 0.9% was used as the vehicle to dissolve the solutions.

After the results obtained in the *in silico* studies, it was observed that of the active compounds ursolic acid (UA) present in the FAc presented better results. Then 6 animals were treated orally with UA (10 mg/kg p.o) and submitted to the carrageenan-induced paw edema test and tail flick.

Carrageenan-Induced Paw Edema

This test was performed to assess the pharmacological activities of the investigated compounds after subplantar injection of carrageenan. Mice were distributed and treated as described in the "Experimental groups" section. Sixty minutes after the onset of treatments, paw edema was induced through administration of 50 μL of 1% carrageenan via subplantar injection in the right paw; the same volume of 0.9% NaCl was injected in the left paw. The paw volume was measured with a digital plethysmometer 1, 2, 3, 4, and 5 h after induction. Edema was calculated as the difference between the right and left paw volume and is expressed as paw volume variation (ml) over time (Winter et al., 1962; Sadeghi et al., 2011).

Writhing Test

The acetic acid-induced writhing test is described as a visceral-somatic inflammatory model used for pharmacological screening of central and peripheral antinociceptive activity. Mice were distributed and treated as described in the "Experimental groups" section. Sixty minutes after treatment onset, abdominal writhing was induced through intraperitoneal administration of 0.8% acetic acid (10 mL/kg). The number of contractions was cumulatively counted for 20 min after induction (Koster et al., 1959). The results are expressed as the average number of cumulative abdominal contractions (Shamsi and Keyhanfar, 2013; Mansouri et al., 2014).

Formalin Test

The formalin test for nociception allows assessment of the neurogenic nociceptive mechanisms triggered by activation of nociceptive fibers and the inflammatory mechanisms activated following the release of inflammatory mediators. Mice were treated as described above; 60 min later, a subplantar injection of 20 μL of 2.5% formalin was administered in the right paw. The nociceptive response, characterized by paw licking or biting, was observed during the first 5 min to assess neurogenic mechanisms and then from minutes 15 to 30 to assess inflammatory mechanisms (Hunskaar and Hole, 1987; Nemoto et al., 2015).

Tail Flick Test

This test was performed to assess central antinociceptive activity through the stimulation of spinal reflexes. Rats were treated as described above; 60 min later, a thermal stimulus was applied to the final third of the tail (Ugo Basile, Varese-Italy), and the latency to tail flick was measured at baseline, 30, 60, 120, and 180 min. The stimulus intensity was set to obtain 3–6 s latency times; the cutoff point was set to 10 s to avoid tail injury (D'Amour and Smith, 1941; Mansouri et al., 2014).

In silico Studies

Structure of Compounds and Receptors

The compounds identified in FAc were obtained from the PubChem Project database and were structurally plotted in 3 dimensions (3D) using GaussView 5.0.8 (Dennington et al., 2009). Geometric and vibrational properties were calculated (optimized) under vacuum by means of the density functional theory (DFT) method using functional hybrid B3LYP combined with basis $6-31 ++ G (d, p)$ in the Gaussian 09 program (Frisch et al., 2009).

The 3D structure of Swiss mouse COX-2 (chain A) was obtained from the Protein Data Bank (PDB, #1DDX). The 3D structures of the drugs MEM and INDO were obtained from the PubChem Project (CID 4054 and 3715, respectively).

The structural model of the *Rattus norvegicus* NMDA receptor subunits GluN1a and GluN2B was obtained by means of homology modeling.

Homology Modeling

Homology modeling was performed following Ramos et al. (2012) with MODELER 9v14 (Webb and Sali, 2014) and the amino acid sequences of subunits GluN1a and GluN2B (NCBI GI 645985944 and GI 645985945, respectively). As the crystallographic structure of the PDB NMDA (code 4PE5) are not complete, models were generated by homology modeling (HM-GluN1a and HM-GluN2B) using the crystallographic structure of PDB code 4TLL (GluN1/GluN2B NMDA) as template. The quality of the selected models was checked with the programs ProCheck (Laskowski et al., 1993) and Errat (Colovos and Yeates, 1993), run in the SAVES server with Z-Score (ProSA-web Protein Structure Analysis) (Table S2).

Molecular Docking

The AutoDock 4.2 package (Morris et al., 2008) was used to prepare proteins (refined models) and ligands for docking calculations using the AutoDock Tools (ADT) module, version 1.5.6, according to Ramos et al. (2012). The affinity grid centers were defined on residue Arg120 for COX-2, Tyr513 for NMDA GluN1A and Arg487 for NMDA GluN2B. The initial complex coordinates for MD simulations were selected based on the lowest energy configuration of clusters combined with visual inspection.

Molecular Dynamics of Complexes

The MD simulations of the complexes selected after molecular docking were performed using GROMACS 4.6.7 software (Berk et al., 2014) following Ramos et al. (2012). The ligand topologies were generated with *Automated Topology Builder* (ATB) *and Repository* version 2.1 (Malde et al., 2011). The protonation states of histidine residues were determined using the H++ online server—http://biophysics.cs.vt.edu/hppdetails. php. To enlarge the sample, 3 10-ns MD simulations were performed per complex using different atomic velocities assigned according to the Maxwell distribution. The data generated for the last 4 ns in each simulated system were used for analysis. During the production step, 123 frames were obtained at 100-ps intervals. The details of the interactions were calculated with *LigPlot++* software (Laskowski et al., 1993). A minimum of 50% of contact (total of hydrophobic interactions and hydrogen bonds) in the analyzed frames was defined as a criterion of binding efficacy.

Statistical Analysis

Mean values among experimental groups were compared through univariate analysis of variance (one-way ANOVA) followed by the Newman-Keuls test at $p < 0.05$. The data were analyzed in the terms of means ± standard errors using GraphPad Prism 5 software.

RESULTS

Phenolic and Flavonoid Content Assessment

The concentrations of total phenolic compounds and flavonoids in EHBv were 9.61 and 7.67 mg/mL, respectively.

HPLC UV/Vis Analysis

Gallic acid, ß-sitosterol, glycyrrhetinic acid, ß-amyrin, caffeic acid, coumaric acid, and quercetin were identified in EHBv (**Table 1** and Figure S1). Gallic acid, ursolic acid, caffeic acid, and ellagic acid were identified in FAc (**Table 1** and Figure S2).

GC-MS Analysis

Thirteen components were detected in FAc, corresponding to alcohols, sugars, fatty acids, and flavonoids. The main components found were the sugars D-psicofuranose (10.2%) and glucopyranose (33.47%) and the fatty acid 10-undecenoic acid (15.70%) (**Table 2**).

In vivo Biological Studies

Carrageenan-Induced Paw Edema Test

Subplantar injection of carrageenan induced edema on the animals' paws that lasted the full period of observation, i.e., 5 h, with the peak of edema starting 4 h after induction.

Treatments consisting of EHBv 500 and FAc (FAc 25 and FAc 50) significantly reduced carrageenan-induced edema at 3, 4, and 5 h after induction compared to control. The percentage of reduction in edema caused by the treatment was 41, 42, and 43% for EHBv 500; 48, 61, and 67% for FAc 25; and 41, 53, and 61% for FAc 50 respectively. Treatment with INDO significantly reduced edema by 72, 74, and 77%, while MEM reduced edema by 20, 18, and 14% at 3, 4, and 5 h after induction, respectively, compared to control. Comparisons between the effects of *B. verticillata* extract, fractions and standard drugs (indomethacin and memantine) revealed that INDO, FAc 25, and FAc 50 were the most efficacious in reducing edema. The effects of FAc at doses of 25 and 50

TABLE 1 | High-performance liquid chromatography (HPLC-UV) analysis of the hydroalcoholic extract (EHBv) and ethyl acetate fraction (FAc) from *B. verticillata*.

	Compounds identified	Retention time (Rt) minute	Area (%)
EHBv	Gallic acid	9.6	1.1
	β-sitosterol	12.9	0.1
	Glycyrrhetinic acid	13.9	1.9
	β- amyrin	14.2	26.6
	Caffeic acid	16.4	0.1
	Coumaric Acid	20.0	1.2
	Quercetin	31.7	14.40
FAc	Gallic acid	4.7	7.3
	Ursolic acid	6.3	2.3
	Caffeic acid	6.71	2.3
	Ellagic acid	8.20	6.1

mg/kg were equivalent, without statistically significant difference (**Figure 1** and Table S1).

Writhing Test

Intraperitoneal administration of acetic acid caused pain to animals during entire 20 min of assessment. Treatments with EHBv 500, FAc 25, and FAc 50 significantly reduced the number of abdominal contractions by 71, 72, and 42%, respectively, compared to control (**Figure 2**). Treatment INDO and MEM significantly reduced the number of abdominal contractions by 72.5 and 33%, respectively, compared to control. The effects of INDO, EHBv 500 and FAc 25 on writhing test, and the reductions in abdominal contractions induced by FAc 50 and MEM were equivalent.

Formalin Test

This test assessed pain at 2 different stages. In stage 1 MEM, FAc 25, and FAc 50 treatments significantly reduced neurogenic pain by 54, 45, and 57%, respectively, compared to control, while INDO did not induce a significant reduction of neurogenic

pain. The effects of FAc 50 and MEM were similar. In stage 2, INDO, MEM, EHBv 500, FAc 25, and FAc 50 treatments significantly reduced inflammatory pain by 82, 63, 57, 57, and 59%, respectively, compared to control (**Figure 3**). The effects of EHBv 500, FAc 25 and FAc 50 were similar to MEM and INDO treatments, without statistically significant differences.

Tail Flick Test

Treatment with MEM significantly reduced pain, as evidenced by 15, 40, and 40% increases in the latency time at 60, 120, and 180 min, respectively, compared to control. INDO, EHBv 500, FAc 25, and FAc 50 were unable to increase the latency time of the animals during the 180 min assessment period (**Figure 4**).
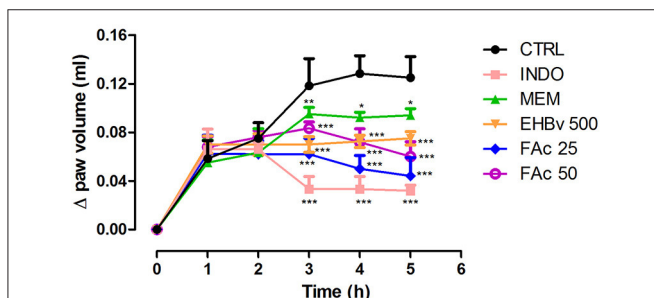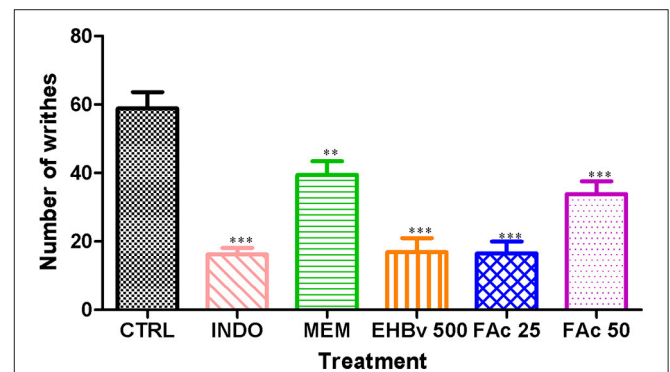
In silico Studies
Molecular Docking

All compounds identified in FAc on HPLC UV-Vis analysis were selected for molecular docking. The parameters affinity (binding energy [ΔG_{bind}] and inhibition constant [Ki]) and values of all ligands are described in **Table 3**.

TABLE 2 | Gas chromatography-mass spectrometry (GC-MS) analysis of the ethyl acetate fraction (FAc) from *B. verticillata*.

Class Component	Compounds identified	Area (%)
Alcohol	Glycerol	9.7
	Butanetriol	3.0
Sugars	D-galactose	1.5
	Trehalose	1.8
	Fructopyranose	2.4
	D-psicofuranose	10.2
	Glucopyranose	33.4
Fatty acids	Palmitic acid	2.0
	Stearic acid	2.7
	1-monopalmitin	2.2
	Acid 10-undecenoic	15.7
Flavonoids	Quercetin	1.9
	Myricetin	2.1

FIGURE 2 | Writhing induced by the intraperitoneal administration of 0.8% acetic acid (10 ml/kg) in mice treated orally with NaCl 0.9%, indomethacin 10 mg/kg, memantine 10 mg/Kg, EHBv 500 mg/Kg and FAc (25 mg/kg and 50 mg/Kg). **p < 0.01; ***p < 0.001 vs. CTRL (ANOVA; Newman Keuls).


FIGURE 1 | Paw edema induced by subplantar administration of 1% carrageenan in mice treated orally with NaCl 0.9%, indomethacin 10 mg/kg, memantine 10 mg/Kg, EHBv 500 mg/Kg and FAc (25 and 50 mg/Kg). *p < 0.05; **p < 0.01; ***p < 0.001 vs. CTRL (ANOVA; Newman Keuls).
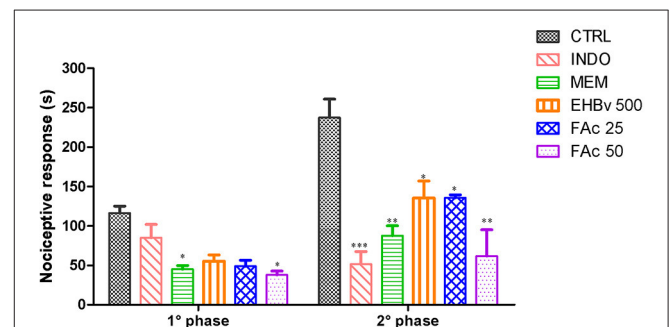
FIGURE 3 | Formalin test induced by subplantar formalin administration of 2.5% in mice treated orally with NaCl 0.9%, indomethacin 10 mg/kg, memantine 10 mg/Kg, EHBv 500 mg/Kg and FAc (25 and 50 mg/Kg). *p < 0.05; **p < 0.01; ***p < 0.001 vs. CTRL (ANOVA; Newman Keuls).
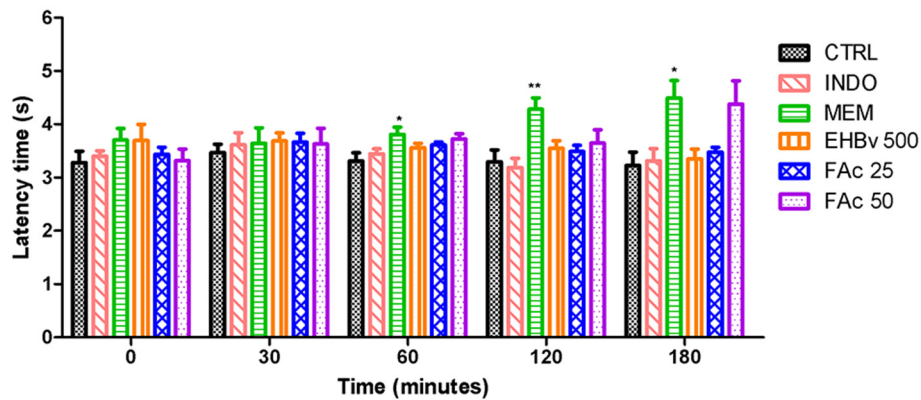
FIGURE 4 | Tail flick test in rats treated orally with NaCl 0.9%, indomethacin 10 mg/kg, memantine 10 mg/Kg, EHBv 500 mg/Kg and FAc (25 mg/kg and 50 mg/Kg). $*p < 0.05$; $**p < 0.01$ vs. CTRL (ANOVA; Newman Keuls).

TABLE 3 | Interactions by molecular docking of indomethacin, memantine and compounds identified in FAc with COX-2, GluN1a and GluN2B.

GluN1a			GluN2B			COX-2		
Ligand	ΔG_{bind}* (kcal/mol)	Ki** (μM)	Ligand	ΔG_{bind} * (kcal/mol)	Ki ** (μM)	Ligand	ΔG_{bind}* (kcal/mol)	Ki** (μM)
Memantine	−7.82	1.86	Memantine	−5.66	71.18	Indomethacin	−8.30	0.82
Ursolic acid	−7.02	7.13	Ursolic acid	−5.69	67.35	Ursolic acid	−9.86	0.05
Ellagic acid	−5.67	70.17	Ellagic acid	−5.34	122.58	Ellagic acid	−7.54	2.99
Gallic acid	−4.57	448.26	Gallic acid	−5.16	164.28	Gallic acid	−6.68	12.69
Caffei acid	−4.47	531.44	Caffei acid	−5.04	201.80	Caffei acid	−5.88	49.19

*ΔG_{bind}, binding energy. **Ki, inhibition constant.

In relation to COX-2, UA exhibited higher ΔG_{bind} values and inhibition constants compared with INDO, which were −9.86 kcal/mol and 0.05 μM and −8.30 kcal/mol and 0.82 μM, respectively. The ΔG_{bind} values corresponding to ellagic acid, caffeic acid, and gallic acid were −7.54, −6.68, and −5.88 kcal/mol, respectively. Relative to the NMDA receptor, UA exhibited the best affinity parameters with GluN1a, with values of −7.02 kcal/mol and 7.13 μM, close to the values obtained for MEM, which were −7.82 kcal/mol and 1.86 μM. With respect to GluN2B, the affinity values of UA were slightly higher compared with MEM, which were −5.69 kcal/mol and 67.35 μM vs. −5.66 kcal/mol and 71.18 μM, respectively. Relative to GluN1a and GluN2B, the ΔG_{bind} values corresponding to ellagic acid, caffeic acid and gallic acid were −5.67, −4.57, and −4.47 kcal/mol and −5.34, −5.16, and −5.04 kcal/mol, respectively.

The interactions of UA, MEM, and INDO with amino acids identified in selected configurations obtained through molecular docking calculations are described in **Table 4**.

Molecular Dynamics Simulations

The lowest docking-energy conformation of the cluster with lowest energy was chosen as initial structure for the molecular dynamics simulations of the COX-2 (**Figures 5A–C**) GluN1a (**Figure 6A** and Figure S3) and GluN2B (**Figure 6B** and Figure S4) (UA, INDO or MEM) complexes. Interactions ≥50% were considered to be relevant.

In relation to COX-2, UA exhibited high frequencies of interaction with Lys79, Leu80, Lys83, Pro84, Arg120, Leu123, Trp155, Ser199, Phe470, Leu472, Ser481, and Glu524 (**Figure 7A**). The highest frequencies of interaction corresponded to Glu524, with 97% of hydrogen bonds, and Arg120, with 96% of hydrophobic interactions. INDO exhibited high frequencies of interaction with Asn43, Arg44, Thr62, Phe64, Leu80, Trp122, Leu123, lle124, Asp125, Phe470, and Arg469; the most relevant interactions corresponded to Trp122 and Leu123, both with 88% of hydrophobic interactions (**Figure 7B**).

With respect to (**Figure 8A**), UA exhibited high frequencies of interaction with lle497, Pro510, Ala502, Phe507, and Glu506, with the highest frequencies being 82% with Ile497 (67% of hydrophobic interactions and 15% of hydrogen bonds) and 81% with Phe507 (24% of hydrophobic bonds and 57% of hydrogen bonds). Relative to GluN2B (**Figure 8B**), UA exhibited high frequencies of interaction with lle483, Ser488, Phe493, Asp492, and Pro496. The frequencies of interaction with Asp492 and Phe493 were both 66%, corresponding to 2 and 25% of hydrophobic bonds and 64 and 41% of hydrogen bonds, respectively. MEM had maximum contact with GluN1a (**Figure 8C**) and high frequencies of interaction with Phe436, Phe511, Lys512, Ala712, Phe736, Glu764, Met763, and Leu766, with 100% of hydrogen bonds with Lys512 and 84% of interactions with Glu764 (61% of hydrophobic interactions and 23% of hydrogen bonds). Regarding to GluN2B

TABLE 4 | Interactions of ursolic acid, memantine and indomethacin for the conformations chosen by molecular docking.

Ligand	GluN1a		GluN2B		COX-2	
	Hydrogen bonds	Hydrophobic interactions	Hydrogen bonds	Hydrophobic interactions	Hydrogen bonds	Hydrophobic interactions
Ursolic acid	Tyr535, Arg733	Ile497, Phe507, Ser508, Lys509, Pro510, Ser734, Gly735	Phe493, Lys736	Ile483, Ser420, Glu489, Val491, Asp492	Lys83, Tyr122, Ser471	Pro84, Tyr115, Ser119, Arg120, Leu123, Phe470, Glu524, Pro528
Memantine	Asp765, Asp767	Lys512, Ala712, Glu715, Phe716, Glu764	Val490	Val169, Trp171, Glu489, Lys736, Asp737	NA	NA
Indomethacin	NA	NA	NA	NA	Lys83, Tyr122	Asn43, Arg44, Thr62, Leu80, Lys468, Arg469, Ser471.

NA, Not rated.

(**Figure 8D**), MEM exhibited 50% interaction with Glu489 (30% of hydrophobic interactions and 20% of hydrogen bonds).

The frequencies of interaction of UA and MEM with GluN1a and GluN2B are described in **Figure 8**.

Test *In vivo* of *In silico* Selected Compound

After analysis of the results obtained from the *in silico* tests, tests of Carrageenan-induced paw edema and Tail flick with UA (Sigma-Alderich) were performed.

Treatment with UA (10 mg/kg) significantly reduced carrageenan-induced edema by at 5 h analyzed. These reductions were 57–84% when compared to the control group. Comparisons of the effects UA, INDO, and MEM revealed that UA were most efficacious in reducing edema. Treatment with INDO and of MEM reduced significantly the paw edema in the 3, 4, and 5 h when compared with CTRL. These reductions were similar to those mentioned above (**Figure 9**).

In tail flick test, treatment with UA (10 mg/kg) significantly increased the animal latency time at 30–120 min at 28–42% when compared to control. This effect was not observed after 180 min. Treatment with MEM significantly increased latency time when compared to control. These results were similar to those mentioned above (**Figure 10**).

DISCUSSION

The assays performed in the present study showed that *B. verticillata* had peripheral antinociceptive effects and anti-inflammatory properties. The *in silico* tests indicated that UA was chief among the active components identified in FAc, exhibiting relevant interactions with amino-acid residues in COX-2 and NMDA receptor active sites.
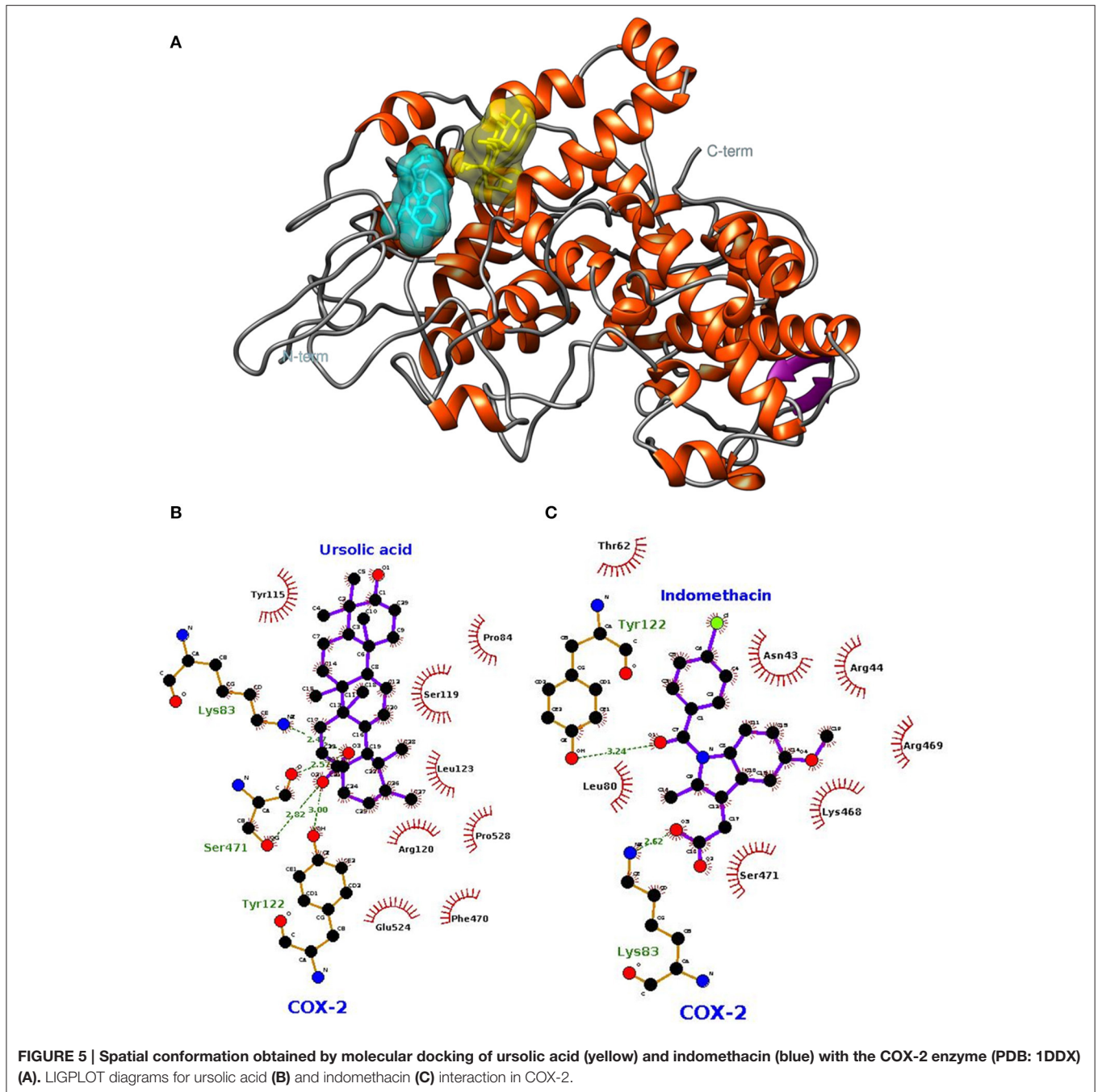
The FAc doses (25 and 50 mg/kg) used in this study were chosen according to results obtained in previous studies developed by our research group. Our preliminary studies with EHBv demonstrated that doses 250 and 500 mg/kg had an antinociceptive effect. In order to define the doses used in FAc, we reduced the EHBv dose by 100 times, resulting in doses of 25 and 50 mg/kg.

The anti-edematous effects of EHBv 500, FAc 25, and FAc 50 were similar to INDO starting 3 h after induction. Studies have shown that the paw edema test has a maximum parameter in 3–4 h lasting up to 5 h. After this period of time, induction loses its effectiveness and due to this reason we do not continue the evaluation (Eisenberg et al., 1994; Castardo et al., 2008). Paw edema characteristically develops in 2 stages: the first stage begins with carrageenan administration and lasts up to 2 h, corresponding to the exudative phase of inflammation, which is triggered by the release of inflammatory mediators such as histamine, serotonin and bradykinin. The second stage begins 3 h after carrageenan administration and is characterized by neutrophil infiltration and is sustained by prostanoids (Wilches et al., 2015; Honmore et al., 2016). Along the inflammatory process, or when tissue damage occurs, several substances are released that promote vasodilation, plasma extravasation and cell recruitment. In addition, glutamate release by primary afferent fibers (class Aδ and C) is increased, as is the activation of glutamatergic receptors, such as NMDA, with consequent propagation of action potentials and the release of excitatory neurotransmitters in the posterior horn of the spinal cord (Miller et al., 2011). Accordingly, the anti-edematous effect of *B. verticillata* FAc might be attributed to COX-2 inhibition and the consequent reduction of PGE_2 synthesis, as it also occurs in the case of oral treatment with INDO. In addition, previous studies showed that blockade of the NMDA receptor also influences inflammation, as it reduces leukocyte migration (Bong et al., 1996) proinflammatory cytokine induction (Morel et al., 2013) and partially inhibits enzyme phospholipase A_2 (Buritova et al., 1996); all of which explain the anti-edematous effect of MEM.

The EHBv 500, FAc 25, and FAc 50 treatments reduced the number of abdominal contractions on the writhing test by 71, 72, and 42%, respectively. The effects of EHBv 500 and FAc 25 were equivalent to INDO and the effect of FAc 50 was equivalent to MEM.

The writhing test is a visceral inflammatory pain model used for screening compounds with peripheral analgesic activity; it involves activation of somatic and visceral receptors in addition to induction of local inflammation mediated by prostaglandins, bradykinin, tumor necrosis factor (TNF) α and interleukins (ILs) 1β and 8 (Rodrigues et al., 2012; Olonode et al., 2015). Some studies have demonstrated increased activation of peripheral receptors and elevated spinal cord glutamate concentrations

FIGURE 5 | Spatial conformation obtained by molecular docking of ursolic acid (yellow) and indomethacin (blue) with the COX-2 enzyme (PDB: 1DDX) (A). LIGPLOT diagrams for ursolic acid **(B)** and indomethacin **(C)** interaction in COX-2.
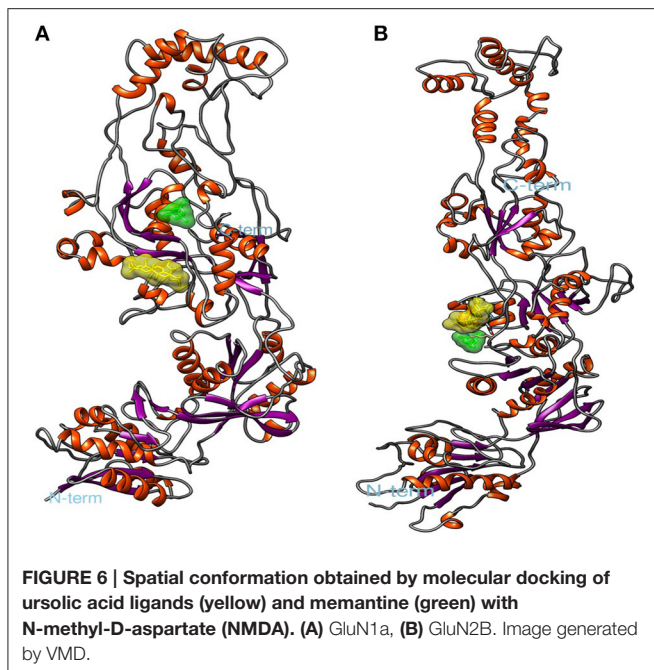
in inflammatory pain models (Santos et al., 2005; Shamsi and Keyhanfar, 2013). As the effects of EHBv 500 and FAc 50 treatments were equivalent to INDO, the results of the present study might be mainly attributed to COX-2 inhibition and the consequent reduction of PGE_2 synthesis. In addition, we must also bear in mind the peripheral inhibition of the action of glutamate on nociceptors induced by MEM, as the effects of this drug and FAc 50 were equivalent.

The results of the present study showed that oral treatment with MEM, FAc 25, and FAc 50 reduced the nociceptive response

in both phases of the formalin test. Treatments with EHBv and INDO reduced the nociceptive response time only in the inflammatory phase. The reductions in the nociceptive response induced by *B. verticillata* extract and FAc were similar to MEM and INDO in the first and second phases of formalin test, respectively.

The formalin-induced nociception model involves a biphasic nociceptive response. The first phase (0–5 min) is neurogenic, when class C fibers are predominantly activated; the second phase (15–30 min) corresponds to inflammation and depends

FIGURE 6 | Spatial conformation obtained by molecular docking of ursolic acid ligands (yellow) and memantine (green) with N-methyl-D-aspartate (NMDA). (A) GluN1a, (B) GluN2B. Image generated by VMD.

on a combination of inflammatory mediators and peripheral and central sensitization (Hunskaar and Hole, 1987; Tjolsen et al., 1992; Liberato et al., 2003).

Peripheral NMDA receptors contribute to the triggering and maintenance of peripheral sensitization under conditions characterized by cell damage and inflammation (Christoph et al., 2005). Several studies have shown that NMDA antagonists, such as MEM, are able to reduce the nociceptive response during both the first and second phases (Davidson and Carlton, 1998; Liberato et al., 2003). McRoberts et al. (2011) found a 50% reduction of the inflammatory phase in GluN1-knockout rats, which suggests that reduced expression of the NMDA receptor decreases glutamate- and substance-P-mediated synaptic signaling in the spinal cord.

NSAIDs such as INDO decrease nociception in the second phase of the nociceptive response only (Tjolsen et al., 1992). On those grounds, one might attribute the reduction of nociception in the first phase to the inhibition of the peripheral action of glutamate on nociceptors and, in the second phase, inhibition of COX-2 and PGE_2 synthesis.

The tail flick test was performed in the present study to investigate the central analgesic potential of EHBv and FAc. The EHBv 500, FAc 25, FAc 50, and INDO treatments were not able to promote central analgesia. In turn, the latency periods were longer (60, 120, and 180 min after treatment, respectively) than with 10 mg/kg MEM. According to Danneman et al. (1994), the tail behavioral response to nociceptive stimuli is predominantly regulated by spinal and supraspinal structures. Thus, the analgesic effect of MEM is due to the blockade of the NMDA receptor, with consequent reduction of central sensitization mediated by excitatory neurotransmitters, such as glutamate (Parsons et al., 1999; Morel et al., 2013).

The absence of the dose-dependent effect can be explained by reducing the dissolution of the higher dose and the fact that

probably the largest dose does not have the same amounts of active compounds present at the lowest dose.

On the basis of *in vivo* tests results, a peripheral antinociceptive activity of *B. verticillata* can be attributed to a reduction in the activity of COX-2 and the peripheral NMDA receptor. In addition the peripheral antinociceptive activity of *B. verticillata* detected in the present study agrees with the findings described by Abdullahi-Gero et al. (2014b). In that study, oral and intraperitoneal treatments with the ethanolic extract of *B. verticillata* leaves in doses of 200–1,000 mg/kg exhibited peripheral and central analgesic and anti-inflammatory effects; furthermore, the results suggested that the 50% lethal dose (LD_{50}) for mice and rats is ≥5,000 mg/kg.
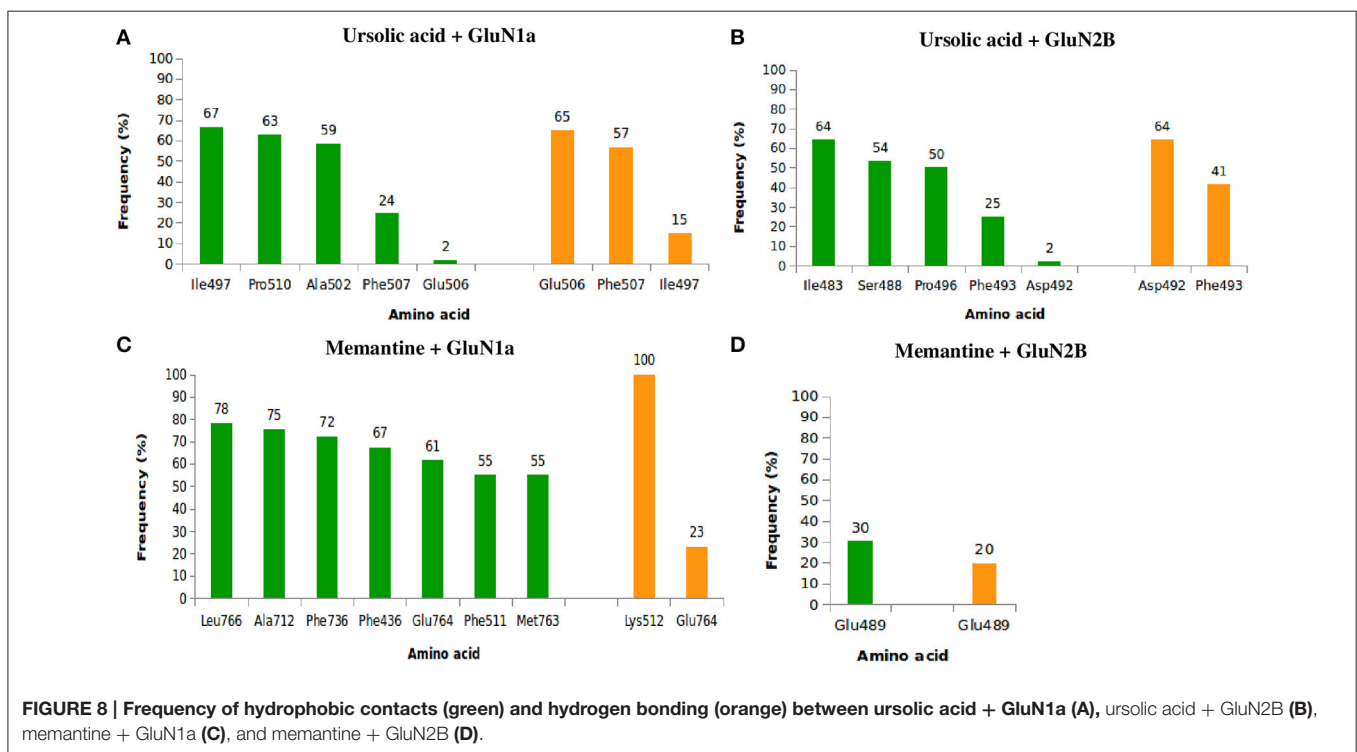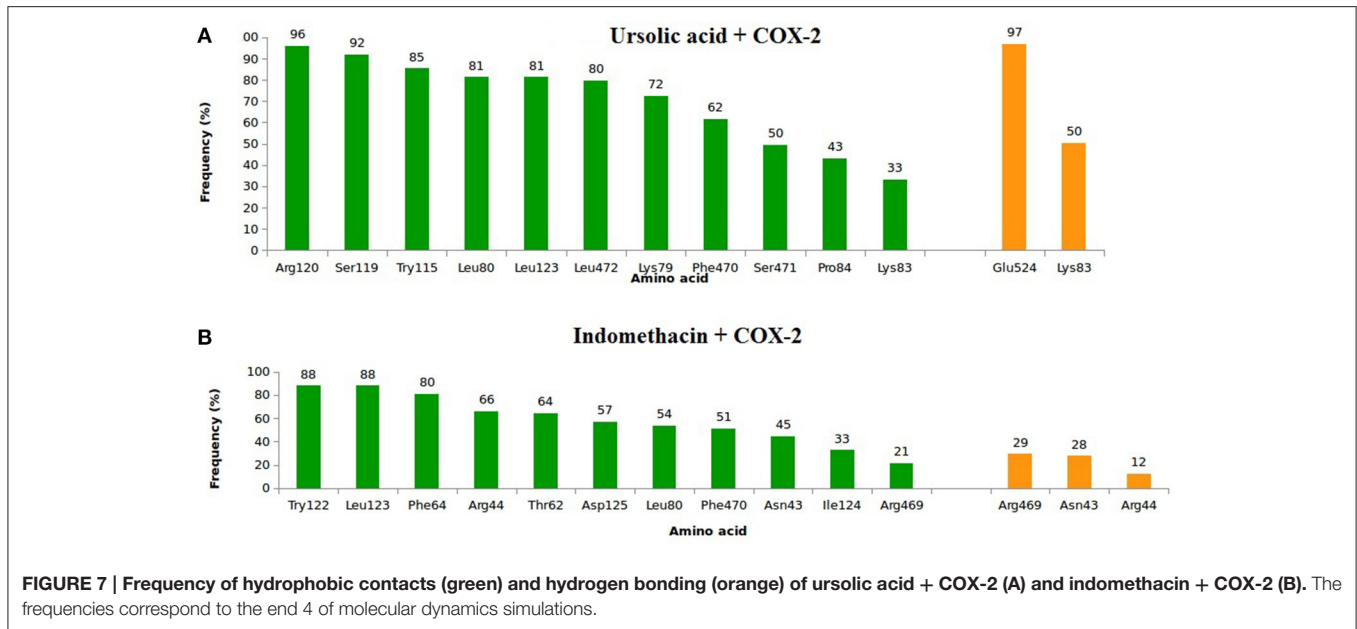
According to the chemical analysis results, the biological activity of *B. verticillata* might be mainly attributed to phenolic compounds and triterpenes, since constituents of these metabolite classes were identified in EHBv and FAc. Some studies showed that these compounds have anti-inflammatory and analgesic effects, as follows: gallic acid—reductions in allodynia and anti-inflammatory effects (Angélica et al., 2013); caffeic acid—reductions in leukocyte migration and free radical and nitric oxide production (Mehrotra et al., 2011); ellagic acid—interaction with opioid receptors (Mansouri et al., 2014) and UA—inhibition of nuclear factor-kappa B (NF-kB) activity (Takada et al., 2010).

In order to determine the mechanisms and possible multi-targets of the peripheral antinociceptive activity of *B. verticillata*, the compounds identified in the FAc were submitted to *in silico* studies. Gallic acid, caffeic acid, ellagic acid, and UA were subjected to molecular docking analysis, targeting COX-2, and NMDA receptor.

According to Guimarães et al. (2014), negative ΔG_{bind} values represent favorable interactions of the ligand-receptor complex. The molecular docking interactions in **Table 3** demonstrated that UA had lower binding energies with the NMDA receptor subunits GluN1a (−7.02 kcal/mol), GluN2B (−5.69 kcal/mol) and COX-2 (−9.89 kcal/mol). Therefore, the UA was the ligand that presented better interactions with the NMDA receptor and COX-2, hence it was selected for MD simulations and *in vivo* tests.

UA interacted with COX-2 and both NMDA receptor subunits as well as the standard drugs INDO and MEM. From a structural point of view, the COX-2 active site consists of a lipophilic channel with a gate formed by residues Arg120, Tyr355, and Glu524 (Rowlinson et al., 2003), and its activation leads to metabolic changes in arachidonic acid (AA) based on interactions with COX-2 residues Arg120, Tyr355, Tyr385, and Ser530, resulting in prostaglandin production (Xu et al., 2014).

Several studies have confirmed the relevance of interactions involving the aforementioned amino acids, thus pointing to them as potential targets in the investigation of COX-2 inhibitors. Fenamic acid derivatives were assessed for COX-2 inhibitory actions *in vitro*; once the efficacy of the compounds was established, the complexes were subjected to x-ray crystallography. The results indicated interactions of fenamic acid derivatives with Arg120, Tyr355, Tyr385, Trp387, Glu524, and Leu531 (Orlando and Malkowski, 2016). *In vitro*

FIGURE 7 | Frequency of hydrophobic contacts (green) and hydrogen bonding (orange) of ursolic acid + COX-2 (A) and indomethacin + COX-2 (B). The frequencies correspond to the end 4 of molecular dynamics simulations.

FIGURE 8 | Frequency of hydrophobic contacts (green) and hydrogen bonding (orange) between ursolic acid + GluN1a (A), ursolic acid + GluN2B **(B),** memantine + GluN1a **(C),** and memantine + GluN2B **(D).**

evaluation of the COX-2 inhibitory potential of meloxicam and isoxicam followed by x-ray crystallography detected interactions of both compounds with Met113, Leu117, Arg120, Ile345, Val349, Leu352, Leu359, Phe518, Ala527, Ser530, and Leu531 (Xu et al., 2014). The interaction of COX-2 with ibuprofen, another NSAID with anti-inflammatory and analgesic activities, involved the participation of COX-2 residues Arg120, Val349, Tyr355, Trp387, Met522, Val523, Gly526, Ala527, and Ser530 (Orlando et al.,

2015). The results of that study further showed that residues Arg120 and Tyr355, located in the COX-2 channel gate, are crucial for the enzyme's interaction with ibuprofen.

Constant interactions between UA and significant amino acid residues, such as Arg120, Glu524, and others closed related to residues described in previous studies, such as Trp115 (close to Met113 and Leu117, involved in meloxicam and isoxicam interactions), Leu123 (close to Arg120, involved in meloxicam,
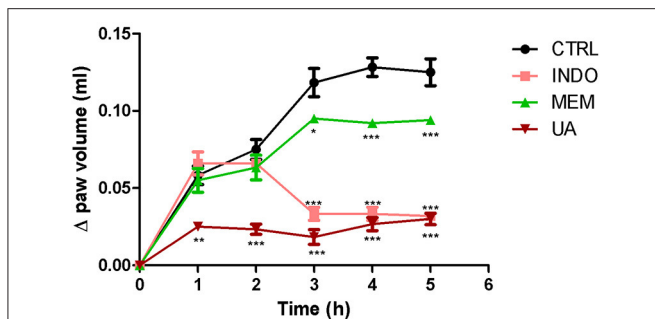
FIGURE 9 | Paw edema induced by subplantar administration of 1% carrageenan in mice treated orally with NaCl 0.9%, indomethacin 10 mg/kg, memantine 10 mg/Kg, and ursolic acid 10 mg/Kg. *$p < 0.05$; **$p < 0.01$; ***$p < 0.001$ vs. CTRL (ANOVA; Newman Keuls).
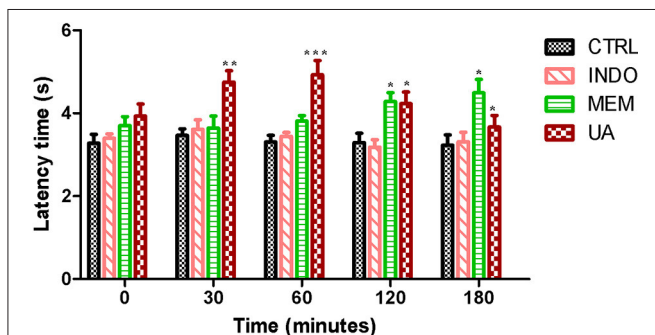
FIGURE 10 | Tail flick test in rats treated orally with NaCl 0.9%, indomethacin 10 mg/kg, memantine 10 mg/Kg, and ursolic acid 10 mg/Kg. *$p < 0.05$; **$p < 0.01$; ***$p < 0.001$ vs. CTRL (ANOVA; Newman Keuls).

isoxicam and ibuprofen interactions), and Glu524 (close to Val523, involved in meloxicam and ibuprofen interactions, and to Gly526, involved in ibuprofen interactions).

The present study further found that the UA and COX-2 interaction profile detected upon molecular docking persisted in the MD simulations, even in the presence of temperature, pressure, water, and protein flexibility variations. In addition, the interactions of UA with amino acid residues adjacent to the COX-2 active site and the AA metabolism site, such as Tyr115, Ser119, Tyr122, Leu123, Asp125, and Pro528, might also intensify the COX-2 inhibitory potential of UA. On the basis of the referred facts: (1) UA might block the access of ligands to the COX-2 active site; (2) interactions with Arg120 and amino acid residues adjacent to the COX-2 active site might reduce arachidonic acid metabolization; and (3) interactions of COX-2 active site inhibitors with Arg120 and Glu524 have already been described, which demonstrates the relevance of these amino acid residues for the possible blocking of the COX-2 active site by UA (Figure S5).

From a structural point of view, the NMDA receptor is a heterotetramer formed by 2 subunits, GluN1 and GluN2. These subunits are modulated by domains ATD, LBD, TMD, and CTD (Karakas and Furukawa, 2014). Activation of the NMDA receptor

requires simultaneous binding of glutamate to GluN2 and glycine or d-serine to GluN1 through the interactions of the latter α-amino and α-carboxyl groups with LBD regions. The LBD is formed by 3 transmembrane regions (M1, M2, and M3) and 2 segments (S1 and S2), which comprise the active site and are located in subdomains D1 and D2, respectively (Traynelis et al., 2010).

According to Kaye et al. (2006), the active site of subdomain D1 is formed by amino acid residues Gln405, Phe484, Thr486, Pro516, Thr518, and Arg523, and the active site of subdomain D2 is formed by Ser688, Ser687, Val6869, Trp731, Asp732, and Ser756. Several studies with GluN1 antagonists, such as 5,7-dichlorokynurenic acid (DCKA) and 1-thioxo-1,2-dihydro-[1,2,4]triazolo[4,3-a]quinoxalin-4(5H)-one (TK40), verified interactions with Phe484, Thr518, Pro516, and Arg523 (Furukawa and Gouaux, 2003) for DCKA and with Glun405, Phe484, Pro516, Leu517, Thr518, Arg523, Ser687, Ser688, and Val689 for TK40 (Kvist et al., 2013). These interactions correspond to residues Gln383, Phe462, Pro494, Leu495, Thr496, Arg501, Ser665, Ser666, and Val667 in our structure. After 10 ns MD simulations, we found high frequencies of interactions of UA with lle497, Ala502, Phe507, Ser508, Lys509, and Pro510, located close to the sites indicated by previous authors, which points to the potential of UA to inhibit glycine binding to GluN1.

Lee et al. (2014) developed a crystallographic structure of GluN2B complexed with the partial agonist trans-1-aminocyclobuthane-1,3-dicarboxylic acid (t-ACBD). Those authors revelead that t-ACBD interacted with the amino acid residues His479 and Thr507, which are equivalent to His454 and Thr482 in the present study. Addicionally, UA presented interactions with Ile483, Ser48, and all other neighboring amino acid residues, thus demonstrating that UA might prevent binding of agonists to the NMDA receptor GluN2B subunit.

Through *in silico* tests was demonstrated that UA has the COX-2 enzyme and NMDA receptor as multi-targets. The interactions of UA with these two pharmacological targets suggest that there is inhibition of COX-2 activation, NMDA receptor and consequently reduction of the painful process. Compounds and multi-target drugs are currently a promising alternative for the treatment of complex and multifactorial pathologies. They present advantages over polypharmaceutical therapies such as: patient adherence to treatment, improved kinetics and therapeutic efficacy, increased therapeutic range, reduction of drug interactions, adverse and toxicological effects (Talevi, 2015; Nicolik et al., 2016). Because UA has exhibited this feature (multi-targets), it may be considered an advantage over other compounds described in the literature. Verano et al. (2013) has shown that UA 10 mg/kg (i.p) has an antinociceptive effect, so we chose this dose to test its effect orally and have confirmed the antinociceptive and anti-inflammatory effects of UA through inhibitions of the TRPV1 receptor and serotonergic synergism (5-HT); reduced IL-2, IL-6, interferon (IFN)-γ, TNF-α, reactive oxygen species (ROS), phospholipase A2 and NF-κβ release; reduced COX-2 and inducible nitric oxide synthase (iNOS) expression; (Kashyap et al., 2016) and favorable interactions for complexes formed with COX-1 and COX-2 (Magalhães et al., 2012). Zhang et al. (2013) demonstrated that UA can induce

apoptosis of cancer cells by reducing COX-2 expression and Ma et al. (2014) demonstrated that UA reduced COX-2 expression in CCl_4-treated animals. The results presented here evidenced that UA exerts peripheral antinociceptive effect by inhibiting COX-2 in carrageenan-induced paw edema test and analgesic central in the tail flick test.

Until now there are no studies performed *in vivo* or *in silico* to analyse the antinociceptive potential of compounds present in the aerial parts of *B. verticillata*. We suggest that the peripheral antinociceptive effect of this plant species is mainly due to actions of anti-inflammatory components. Possibly contributing to reducing the activity of the enzyme COX-2 and peripheral NMDA receptors, with consequent reductions in pain. *In silico* and *in vivo* studies allowed the selection and suggestion of UA as the main active compound in *B. verticillata*, as it exhibited desirable affinity parameters, stable interactions with COX-2 and NMDA receptor subunits GluN1a and GluN2B and presented peripheral and central analgesic effect. Thus, the UA is configured a promising molecule for the development of COX-2 inhibitors and NMDA receptor antagonists.

AUTHOR CONTRIBUTIONS

Conceived and designed the experiments: RS, MC, JD. Methodology: RS, NL, AL, CV, FL, JD, LD, RR. Analyzed the data: RS, AL, CV, JD, LD, RR, MC, JG. Contributed reagents/materials/analysis tools: RR, MR. Wrote the paper: RS, AL, CV, JD, LD, RS, MC, JD.

FUNDING

ACKNOWLEDGMENTS

SUPPLEMENTARY MATERIAL

The Supplementary Material for this article can be found online at: http://journal.frontiersin.org/article/10.3389/fphar. 2017.00283/full#supplementary-material

REFERENCES

Abdullahi-Gero, H. S., Ahmad, A. Z., and Hussaini, I. M. (2014a). Evaluation of antioxidant activity of leave extract of *Borreria verticillta* Linn (Rubiaceae). *J. Nat. Sci. Res.* 9, 25–30.

Abdullahi-Gero, H. S., Ahmed, A., Zezi, A. U., and Hussaini, I. M. (2014b). Preliminary evaluation of ethanol leaf extract of *Borreria verticillata* Linn (Rubiaceae) for analgesic and anti-inflammatory effects. *J. Med. Plant Res.* 20, 736–747. doi: 10.5897/JMPR2014.5450

Angélica, G. C., Candida, A. L. K., João, B. C., and Petrovick, P. R. (2013). Anti-inflammatory, antiallodynic effects and quantitative analysis of gallic acid in spray dried powders from *Phyllanthus niruri* leaves, stems, roots and whole plant. *Rev. Bras. Farmacogn.* 23, 124–131. doi: 10.1590/S0102-695X2012005000133

Balde, A. M., Pietexrs, L. A., Traore, M. S., Camara, A., Balde, M. A., Oulare, K., et al. (2015). Chemotherapeutical evaluation of *Borreria verticillata* extracts. *J. Plant Sci.* 3, 28–31. doi: 10.11648/j.jps.s.2015030102.16

Berk, H., David, S., and Erik, L. (2014). *Gromacs User Manual Version 4.6.7.* Available online at: www.gromacs.org (Accessed April 10, 2016).

Bong, G. W., Rosengren, S., and Firestein, G. S. (1996). Spinal cord adenosine receptor stimulation in rats inhibits peripheral neutrophil accumulation. The role of N-methyl-D-aspartate receptors. *J. Clin. Invest.* 12, 2779–2785. doi: 10.1172/JCI119104

Buritova, J., Chapman, V., Honoré, P., and Besson, J. M. (1996). Interactions between NMDA- and prostaglandin receptor-mediated events in a model of inflammatory nociception. *Eur. J. Pharmacol.* 303, 91–100. doi: 10.1016/0014-2999(96)00074-X

Castardo, J. C., Prudente, A. S., Ferreira, J., Guimarães, C. L., Monache, F. D., et al. (2008). Anti-inflammatory effects of hydroalcoholic extract and two biflavonoids from *Garcinia gardneriana* leaves in mouse paw oedema. *J. Ethnopharmacol.* 3, 405–411. doi: 10.1016/j.jep.2008.05.002

Chen, L., Yang, G., and Grosser, T. (2013). Prostanoids and inflammatory pain. *Prostaglandins Other Lipid Mediat.* 104–105, 58–66. doi: 10.1016/j.prostaglandins.2012.08.006

Christoph, T., Reissmüller, E., Schiene, K., Englberger, W., and Chizh, B. A. (2005). Antiallodynic effects of NMDA glycine(B) antagonists in neuropathic pain: possible peripheral mechanisms. *Brain Res.* 1–2, 218–27. doi: 10.1016/j.brainres.2005.04.081

Colovos, C., and Yeates, T. O. (1993). Verification of protein structures: patterns of nonbonded atomic interactions. *Protein Sci.* 9, 1511–1519. doi: 10.1002/pro.5560020916

D'Amour, F. E., and Smith, D. L. (1941). A method for determining loss of pain sensation. *J. Pharmacol. Exp. Ther.* 72, 74–79.

Danneman, P. J., Kiritsy-Roy, J. A., Morrow, T. J., and Casey, K. L. (1994). Central delay of the laser-activated rat tail-flick reflex. *Pain* 58, 39–44. doi: 10.1016/0304-3959(94)90183-X

Davidson, E. M., and Carlton, S. M. (1998). Intraplantar injection of dextrorphan, ketamine or memantine attenuates formalin-induced behaviors. *Brain Res.* 785, 136–142. doi: 10.1016/S0006-8993(97)01396-6

Dennington, R., Keith, T., and Millam, J. (2009). *GaussView. Version 5.* Shawnee Mission, KS: Semichem Inc.

Dutra, R. P., Abreu, B. V., Cunha, M. S., Batista, M. C., Torres, L. M., Nascimento, F. R. et al. (2014). Phenolic acids, hydrolyzable tannins, and antioxidant activity of geopropolis from the stingless bee *Melipona fasciculata* Smith. *J. Agric. Food Chem.* 12, 2549–2557. doi: 10.1021/jf404875v

Dutra, R. P., Nogueira, A. M. C., Marques, R. R. O., Costa, M. C. P., and Ribeiro, M. N. S. (2008). Avaliação farmacognóstica de geoprópolis de Melipona fasciculata Smith da Baixada maranhense, Brasil. *Rev. Bras. Farmacogn.* 18, 557–562. doi: 10.1590/S0102-695X2008000400010

Eisenberg, E., LaCross, S., and Strassman, A. M. (1994). The effects of the clinically tested NMDA receptor antagonist memantine on carrageenan-induced thermal hyperalgesia in rats. *Eur. J. Pharmacol.* 255, 123–129. doi: 10.1016/0014-2999(94)90090-6

Frisch, M. J., Trucks, G. W., Schlegel, H. B., Scuseria, G. E., Robb, M. A., Cheeseman, J. R., et al. (2009). *Gaussian 09, Revision, D.01.* Wallingford, CT: Gaussian, Inc.

Furukawa, H., and Gouaux, E. (2003). Mechanisms of activation, inhibition and specificity:crystal structures of the NMDA receptor

NR1 ligand-binding core. *EMBO J.* 12, 2873–2885. doi: 10.1093/emboj/cdg303

Guimarães, A. G., Scotti, L., Scotti, M. T., Mendonça, J. F. J., Melo, N. S., Alves, R. S., et al. (2014). Evidence for the involvement of descending pain-inhibitory mechanisms in the attenuation of cancer pain by carvacrol aided through a docking study. *Life Sic.* 116, 8–15. doi: 10.1016/j.lfs.2014.08.020

Hewitt, D. (2000). The use of NMDA-receptor antagonists in the treatment of chronic pain. *Clin. J. Pain.* 16, 77–79. doi: 10.1097/00002508-200006001-00013

Honmore, V. S., Kandhare, A. D., Kadam, P. P., Khedkar, V. M., Sarkar, D., Bodhankar, S. L., et al. (2016). Isolates of *Alpinia officinarum* Hance as COX-2 inhibitors: Evidence from anti-inflammatory, antioxidant and molecular docking studies. *Int. Immunopharmacol.* 33, 8–17. doi: 10.1016/j.intimp.2016.01.024

Hunskaar, S., and Hole, K. (1987). The formalin test in mice: dissociation between inflammatory and non-inflammatory pain. *Pain* 30, 103–114. doi: 10.1016/0304-3959(87)90088-1

Júnior, J. C. F., Lemos, R. P. L., and Conserva, L. M. (2012). Chemical constituents from *Spermacoce verticillata* (Rubiaceae). *Biochem. Syst. Ecol.* 44, 208–211. doi: 10.1016/j.bse.2012.05.011

Kandimalla, R., Kalita, S., Saikia, B., Choudhury, B., Singh, Y. P., Kalita, K., et al. (2016). Antioxidant and hepatoprotective potentiality of *Randiadu metorum* Lam. leaf and bark via inhibition of oxidative stress and inflammatory cytokines. *Front. Pharmacol.* 7:205. doi: 10.3389/fphar.2016.00205

Karakas, E., and Furukawa, H. (2014). Crystal structure of a heterotetrameric NMDA receptor ion channel. *Science* 344, 992–997. doi: 10.1126/science.1251915

Kashyap, D., Tuli, H. S., and Sharma, A. K. (2016). Ursolic acid (UA): a metabolite with promising therapeutic potential. *Life Sci.* 146, 201–213. doi: 10.1016/j.lfs.2016.01.017

Kaye, S. L., Sansom, M. S., and Biggin, P. C. (2006). Molecular dynamics simulations of the ligand-binding domain of an N-methyl-D-aspartate receptor. *J. Biol. Chem.* 18, 12736–12742. doi: 10.1074/jbc.M512728200

Koster, R., Anderson, M., and Debeer, E. J. (1959). Acetic acid analgesic screening. *Fed. Proc.* 18, 418–420.

Kvist, T., Steffensen, T. B., Greenwood, J. R., Mehrzad Tabrizi, F., Hansen, K. B., Gajhede, M., et al. (2013). Crystal structure and pharmacological characterization of a novel N-methyl-D-aspartate (NMDA) receptor antagonist at the GluN1 glycine binding site. *J. Biol. Chem.* 46, 33124–33135. doi: 10.1074/jbc.M113.480210

Laskowski, R. A., MacArthur, M. W., Moss, D. S., and Thornton, J. M. (1993). PROCHECK: a program to check the stereochemical quality of protein structures. *J. Appl. Crystallogr.* 26, 283–291. doi: 10.1107/S0021889892009944

Lee, C. H., Lu, W., Michel, J. C., Goehring, A., Du, J., Song, X., et al. (2014). NMDA receptor structures reveal subunit arrangement and pore architecture. *Nature* 511, 191–197. doi: 10.1038/nature13548

Liberato, B., Patrizia, O., Francesco, M., Caterina, A., Sabatino, M., Antonio, G., et al. (2003). Antinociceptive effect in mice of intraperitoneal N-methyl-D-aspartate receptor antagonists in the formalin test. *Eur. J. Pain.* 2, 131–137. doi: 10.1016/S1090-3801(02)00086-1

Ma, J. Q., Ding, J., Zhang, L., and Liu, C. M. (2014). Ursolic acid protects mouse liver against CCl4-induced oxidative stress and inflammation by the MAPK/NF-κB pathway. *Environ. Toxicol. Pharmacol.* 37, 975–983. doi: 10.1016/j.etap.2014.03.011

Magalhães, W. S., Corrêa, C. M., Alencastro, R. B., and Nagem, T. J. (2012). Bases moleculares da ação anti-inflamatória dos ácidos oleanólico e ursólico sobre as isoformas da ciclo-oxigenase por docking e dinβmica molecular. *Química Nova.* 2, 241–248. doi: 10.1590/S0100-40422012000200003

Malde, A. K., Zuo, L., Breeze, M., Stroet, M., Poger, D., Nair, P. C., et al. (2011). An automated force field topology builder (ATB) and repository: Version 1.0. *J. Chem. Theory Comput.* 12, 4026–4037. doi: 10.1021/ct200196m

Mansouri, M. T., Naghizadeh, B., and Ghorbanzadeh, B. (2014). Involvement of opioid receptors in the systemic and peripheral antinociceptive actions of ellagic acid in the rat formalin test. *Pharmacol. Biochem. Behav.* 120, 43–49. doi: 10.1016/j.pbb.2014.02.009

McRoberts, J. A., Ennes, H. S., Marvizón, J. C., Fanselow, M. S., Mayer, E. A., and Vissel, B. (2011). Selective knockdown of NMDA receptors in primary afferent

neurons decreases pain during phase 2 of the formalin test. *Neuroscience* 172, 474–482. doi: 10.1016/j.neuroscience.2010.10.045

Mehrotra, A., Shanbhag, R., Chamallamudi, M. R., Singh, V. P., and Mudgal, J. (2011). Ameliorative effect of caffeic acid against inflammatory pain in rodents. *Eur. J. Pharmacol.* 1–3, 80–86. doi: 10.1016/j.ejphar.2011.05.039

Meng, X. Y., Zhang, H. Z., Mezei, M., and Cui, M. (2011). Molecular docking: a powerful approach for structure-baseddrug discovery. *Curr. Comput. Aided Drug Des.* 7, 146–115. doi: 10.2174/157340911795677602

Miller, K. E., Hoffman, E. M., Sutharshan, M., and Schechter, R. (2011). Glutamate pharmacology and metabolism in peripheral primary afferents: physiological and pathophysiological mechanisms. *Pharmacol. Ther.* 3, 283–309. doi: 10.1016/j.pharmthera.2011.01.005

Morel, V., Etienne, M., Wattiez, A. S., Dupuis, A., Privat, A. M., Chalus, M., et al. (2013). Memantine, a promising drug for the prevention of neuropathic pain in rat. *Eur. J. Pharmacol.* 1–3, 382–390. doi: 10.1016/j.ejphar.2013.06.020

Morris, G. M., Huey, R., and Olson, A. J. (2008). Using AutoDock for ligand-receptor docking. *Curr. Protoc. Bioinformatics* 8, 14. doi: 10.1002/0471250953.bi0814s24

Murtala, Y., Babandi, A., Sunusi, M. M., Shehu, D., Babagana, K., and Alhassan, A. J. (2015). Effect of aqueous leaf extract of *Borreria verticillata* of Sudano-Sehelian Savanna on CCl4 induced hepatotoxicity. *J. Nat. Sci. Res.* 5, 67–72.

Nemoto, W., Ogata, Y., Nakagawasai, O., Yaoita, F., Tanado, T., and Tan-No, K. (2015). The intrathecal administration of losartan, an AT1 receptor antagonist, produces an antinociceptive effect through the inhibiton of p38 MAPK phosphorylation in the mouse formalin test. *Neurosci. Lett.* 585, 17–22. doi: 10.1016/j.neulet.2014.11.018

Neto, P. A. S. P., Vladimilsa, S. M., Corrente, C. N. V., Porfírio, Z., and Caetano, L. C. (2002). Antibacterial activity of *Borreria verticillata* roots. *Fitoterapia* 73, 529–531. doi: 10.1016/S0367-326X(02)00166-1

Nickel, F. T., Seifert, F., Lanz, S., and Maihöfner, C. (2012). Mechanisms of neuropathic pain. *Eur. Neuropsychopharmacol.* 22, 81–91. doi: 10.1016/j.euroneuro.2011.05.005

Nicolik, K., Marvidis, D., Djikic, T., Vucicevic, J., Agbaba, D., Yelekci, K., et al. (2016). Drug design for CNS diseases: Polypharmacological profiling of compounds using cheminformatic, 3D-QSAR and Virtual Screening Methodologies. *Front. Neurosci.* 10:265. doi: 10.3389/fnins.2016.00265

Ogunwande, I. A., Walker, T. M., Bansal, A., Setzer, W. N., and Essien, E. E. (2010). Essential oil constituents and biological activities of *Peristrophe bicalyculata* and *Borreria verticillata*. *Nat. Prod. Commun.* 5, 1815–1818.

Olonode, E. T., Aderibigbe, A. O., and Bakre, A. G. (2015). Anti-nociceptive activity of the crude extract of *Myrianthus arboreus* P. Beauv (Cecropiaceae) in mice. *J. Ethnopharmacol.* 171, 94–98. doi: 10.1016/j.jep.2015.05.005

Orlando, B. J., Lucido, M. J., and Malkowski, M. G. (2015). The structure of ibuprofen bound to cyclooxygenase-2. *J. Struct. Biol.* 189, 62–66. doi: 10.1016/j.jsb.2014.11.005

Orlando, B. J., and Malkowski, M. G. (2016). Substrate-selective inhibition of cyclooxygeanse-2 by fenamic acid derivatives is dependent on peroxide tone. *J. Biol. Chem.* 291, 15069–15081. doi: 10.1074/jbc.M116.725713

Parsons, C. G., Danysz, W., and Quack, G. (1999). Memantine is a clinically well tolerated N-methyl-D-aspartate (NMDA) receptor antagonist a review of preclinical data. *Neuropharmacology* 38, 735–767. doi: 10.1016/S0028-3908(99)00019-2

Phang, L. K. D., and Tan, K. H. (2013). Current pharmacological modalities for control of chronic non-cancer pain. *Trends Anaesth. Crit. Care* 3, 283–288. doi: 10.1016/j.tacc.2013.02.006

Ramos, R. M., Perez, J. M., Baptista, L. A., and de Amorim, H. L. (2012). Interaction of wild type, G68R and L125M isoforms of the arylamine-N-acetyltransferase from *Mycobaerium tuberculosis* with isoniazid: a computational study on a new possible mechanism of resistance. *J. Mol. Model.* 18, 4013–4024. doi: 10.1007/s00894-012-1383-6

Ricciotti, E., and Fitzgerald, G. A. (2011). Prostaglandins and inflammation. *Arterioscler. Thromb. Vasc. Biol.* 31, 986–1000. doi: 10.1161/ATVBAHA.110.207449

Rodrigues, M. R., Kanazawa, L. K., das Neves, T. L., da Silva, C. F., Horst, H., Pizzolatti, M. G., et al. (2012). Antinociceptive and anti-inflammatory potential of extract and isolated compounds from the leaves of *Salvia officinalis* in mice. *J. Ethnopharmacol.* 139, 519–526. doi: 10.1016/j.jep.2011.11.042

Rowlinson, S. W., Kiefer, J. R., Prusakiewicz, J. J., Pawlitz, J. L., Kozak, K. R., Kalgutkar, A. S., et al. (2003). A novel mechanism of cyclooxygenase-2 inhibition involving interactions with Ser-530 and Tyr-385. *J. Biol. Chem.* 46, 45763–45769. doi: 10.1074/jbc.M305481200

Sadeghi, H., Hajhashemi, V., Minaiyan, M., Movahedian, A., and Talebi, A. (2011). A study on the mechanisms involving the anti-inflammatory effect of amitriptyline in carrageenan-induced paw edema in rats. *Eur. J. Pharmacol.* 1–3, 396–401. doi: 10.1016/j.ejphar.2011.05.053

Santos, A. R., Gadotti, V. M., Oliveira, G. L., Tibola, D., Paszcuk, A. F., Neto, A., et al. (2005). Mechanisms involved in the antinociception caused by agmatine in mice. *Neuropharmacology* 7, 1021–1034. doi: 10.1016/j.neuropharm.2005.01.012

Shamsi, M. M., and Keyhanfar, F. (2013). Assessment of the antinociceptive effects of pregabalin alone or in combination with morphine during acetic acid-induced writhing in mice. *Pharmacol. Biochem. Behav.* 110, 249–254. doi: 10.1016/j.pbb.2013.07.021

Sharma, V., and Sarkar, I. N. (2012). Bioinformatics opportunities for identification and study of medicinal plants. *Brief Bioinform.* 14, 238–250. doi: 10.1093/bib/bbs021

Souza, R. K. D., Mendonça, A. C. A. M., and Silva, M. A. P. (2013). Ethnobotanical, phytochemical and pharmacological aspects Rubiaceae species in Brazil. *Rev Cubana Plant Med.* 18, 140–156.

Tajima, N., Karakas, E., Grant, T., Simorowski, N., Diaz-Avalos, R., Grigorieff, N., et al. (2016). Activation of NMDA receptors and the mechanism of inhibition by ifenprodil. *Nature* 534, 63–68. doi: 10.1038/nature17679

Takada, K., Nakane, T., Masuda, K., and Ishii, H. (2010). Ursolic acid and oleanolic acid, members of pentacyclic triterpenoid acids, suppress TNF-α-induced E-selectin expression by cultured umbilical vein endothelial cells. *Phytomedicine* 17, 1114–1119. doi: 10.1016/j.phymed.2010.04.006

Talevi, A. (2015). Multi-target pharmacology: possibilities and limitations of the "skeleton key approach" from a medicinal chemist perspective. *Front. Pharmacol.* 22:205. doi: 10.3389/fphar.2015.00205

Tjolsen, A., Berge, O. G., Hunskaar, S., Rosland, J. H., and Hole, K. (1992). The formalin test: an evaluation of the method. *Pain* 51, 5–17. doi: 10.1016/0304-3959(92)90003-T

Traynelis, S. F., Wollmuth, L. P., McBain, C. J., Menniti, F. S., Vance, K. M., Ogden, K. K., et al. (2010). Glutamate receptor ion channels: structure, regulation, and function. *Pharmacol. Rev.* 62, 405–496. doi: 10.1124/pr.109.002451

Verano, J., González-Trujano, M. E., Déciga-Campos, M., Ventura-Martínez, R., and Pellicer, F. (2013). Ursolic acid from *Agastache mexicana* aerial parts produces antinociceptive activity involving TRPV1 receptors, cGMP and a serotonergic synergism. *Pharmacol. Biochem. Behav.* 110, 255–264. doi: 10.1016/j.pbb.2013.07.020

Vieira, I. J., Mathias, L., Braz-filho, R., and Schripsema, J. (1999). Iridinoids from *B. verticillata*. *Organ Lett.* 1, 1169–1171. doi: 10.1021/ol9 90811b

Webb, B., and Sali, A. (2014). Comparative protein structure modeling using MODELLER. *Curr. Protoc. Bioinformatics* 47, 561–532. doi: 10.1002/0471250953.bi0506s47

Wilches, I., Tobar, V., Peñaherrera, E., Cuzco, N., Jerves, L., Vander, H. Y., et al. (2015). Evaluation of anti-inflammatory activity of the methanolic extract from *Jungia rugosa* leaves in rodents. *J. Ethnopharmacol.* 173, 166–171. doi: 10.1016/j.jep.2015.07.004

Winter, C. A., Risley, E. A., and Nuss, G. W. (1962). Carrageenin-induced edema in hind paw of the rat as an assay for antiiflammatory drugs. *Proc. Soc. Exp. Biol. Med.* 111, 544–547. doi: 10.3181/00379727-111-27849

Xu, S., Hermanson, D. J., Banerjee, S., Ghebreselasie, K., Clayton, G. M., Garavito, R. M., et al. (2014). Oxicams bind in a novel mode to the cyclooxygenase active site via a two-water-mediated H-bonding Network. *J. Biol. Chem.* 10, 6799–6808. doi: 10.1074/jbc.M113.517987

Zaia, M. G., Cagnazzo, T. O., Feitosa, K. A., Soares, E. G., Faccioli, L. H., Allegretti, S. M., et al. (2016). Anti-inflammatory properties of menthol and menthone in *Schistosomamansoni* infection. *Front. Pharmacol.* 7:170. doi: 10.3389/fphar.2016.00170

Zaiss, A. K., Zuber, J., Chu, C., Machado, H. B., Jiao, J., Catapang, A. B., et al. (2014). Reversible suppression of cyclooxygenase 2 (COX-2) expression *in vivo* by inducible RNA interference. *PLoS ONE* 9:e101263. doi: 10.1371/journal.pone.0101263

Zhang, H., Li, X., Ding, J., Xu, H., Dai, X., Hou, Z., et al. (2013). Delivery of ursolic acid (UA) in polymeric nanoparticles effectively promotes the apoptosis of gastric cancer cells through enhanced inhibition of cyclooxygenase 2 (COX-2). *Int. J. Pharm.* 441, 261–268. doi: 10.1016/j.ijpharm.2012. 11.034